Journal of Sound and Vibration (2000) **236**(2), 367–373
doi:10.1006/jsvi.2000.2953, available online at http://www.idealibrary.com on IDEAL®

SCATTERING OF FLEXURAL WAVES FROM A COATED CYLINDRICAL ANOMALY IN A THIN PLATE

VERNON A. SQUIRE AND TONY W. DIXON

Department of Mathematics and Statistics, University of Otago, PO Box 56, Dunedin, New Zealand

1. INTRODUCTION

Although more than 40 years old the study of wave propagation in random media continues to be active, enlivened further in the last decade by the experimental validation of theoretical work that predicts the possibility of strong localization of light [1]. The focus of recent theoretical studies has been the so-called coherent-potential approximation (CPA) applied to wave propagation in a medium that possesses randomly placed, discrete variations in its material properties. Applications governed by the Helmholtz equation have been studied, e.g., quantum, electromagnetic, acoustical, or shallow water wave systems [2]. The present authors have also recently extended CPA theory to systems described by a different wave equation, namely the Euler–Bernoulli equation, which governs the motion of flexural waves on thin plates [3]. It is also planned to apply the technique to the multiple scattering of surface water waves by pack ice floes in the Arctic and Antarctic marginal ice zones, with each floe being regarded as a thin elastic plate.

CPA uses a fictitious "effective medium" to derive the transport properties of a specified random medium. In essence, a new reference frame can be found where multiple-scattering effects vanish on average. The most recent models consider scattering from a "coated scatterer", i.e., a single scatterer surrounded by some of the background medium, embedded in an effective medium, which replaces the remainder of the random medium. The properties of the effective medium, and hence of the original random medium in an averaged sense, must be determined by use of an appropriate criterion [4–8].

To extend the methods used in Helmholtz systems to the Euler–Bernoulli case with flexural waves, it is first necessary to find the scattering coefficients for a coated scatterer. This is done in a similar manner to those derived for electromagnetic wave scattering from a coated sphere [9]. Accordingly, in this note we find the scattering properties of a single, coated cylindrical anomaly located in a thin plate on which flexural waves propagate.

2. THE MODEL

We consider a thin elastic plate of flexural rigidity D, Poisson ratio v, density ρ and thickness h in which a solitary coated cylindrical inhomogeneity exists. An incident plane wave of wave number $k = (\rho h\omega^2/D)^{1/4}$ and radian frequency ω impinges on this inhomogeneity in the x direction. Its displacement can therefore be written as $e^{ikr\cos\theta}$. The coated region is composed of a cylindrical core, designated zone 1, with properties D_1, v_1, ρ_1 and h_1 occupying $r < a$ surrounded by an annulus, designated zone 2, with properties D_2, v_2, ρ_2 and h_2 occupying $a \leqslant r < b$. Wave numbers within zones 1 and 2 are k_1 and k_2 respectively. The configuration is illustrated in Figure 1.

0022-460X/00/370367 + 07 $35.00/0

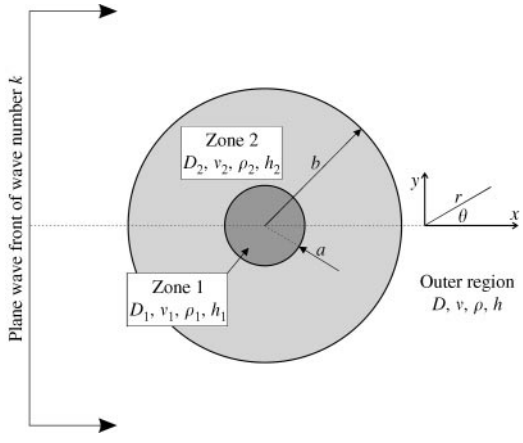

Figure 1. Schematic diagram showing the problem being modelled.

The plate is assumed to be continuous across the $r = b$ boundary but three possible boundary conditions are allowed at $r = a$; continuity, clamped or free. As described below, the solution for the scattered field arising from an incoming plane wave is found in a similar manner to that of Norris and Vemula [10].

By first expanding the incoming wave field $e^{ikr\cos\theta} = \sum_{n=0}^{\infty} \varepsilon_n i^n J_n(kr)\cos n\theta$, $\varepsilon_n = 2$ for $n > 0$, $\varepsilon_0 = 1$, the total displacement can be expanded in terms of sums of various Bessel functions as follows:

$$w = \begin{cases} \displaystyle\sum_{n=0}^{\infty} \varepsilon_n i^n [g_n J_n(k_1 r) + h_n I_n(k_1 r)]\cos n\theta, & r < a, \\ \displaystyle\sum_{n=0}^{\infty} \varepsilon_n i^n [c_n Y_n(k_2 r) + d_n K_n(k_2 r) + e_n J_n(k_2 r) + f_n I_n(k_2 r)]\cos n\theta, & a \leqslant r < b, \\ \displaystyle\sum_{n=0}^{\infty} \varepsilon_n i^n J_n(kr)\cos n\theta + \sum_{n=0}^{\infty} \varepsilon_n i^n [a_n H_n^{(1)}(kr) + b_n K_n(kr)]\cos n\theta, & b \leqslant r. \end{cases} \quad (1)$$

In this expression the factor $\varepsilon_n i^n$ is introduced for convenience so as to match the series for $e^{ikr\cos\theta}$.

2.1. GENERAL PROBLEM

The general problem is defined such that w, $\partial w/\partial r$, M_r and V_r are continuous across the two boundaries at $r = a$ and $r = b$. Here M_r and V_r are, respectively, the radial bending moment and shear, defined in cylindrical polar co-ordinates:

$$M_r = -D\left[\frac{\partial^2 w}{\partial r^2} + \nu\left(\frac{1}{r}\frac{\partial w}{\partial r} + \frac{1}{r^2}\frac{\partial^2 w}{\partial \theta^2}\right)\right].$$

$$V_r = -D\frac{\partial}{\partial r}\nabla^2 w - D(1-\nu)\frac{\partial}{\partial \theta}\left(\frac{\partial^2 w}{\partial r \partial \theta} - \frac{1}{r}\frac{\partial w}{\partial \theta}\right). \quad (2)$$

Continuity is now applied for each value of n in the series to obtain the following system of equations for the unknown coefficients:

$$\begin{bmatrix}
\mathrm{H}_n^{(1)}(kb) & \mathrm{K}_n(kb) & -\mathrm{Y}_n(k_2b) & -\mathrm{K}_n(k_2b) & -\mathrm{J}_n(k_2b) & -\mathrm{I}_n(k_2b) & 0 & 0 \\
0 & 0 & \mathrm{Y}_n(k_2a) & \mathrm{K}_n(k_2a) & \mathrm{J}_n(k_2a) & \mathrm{I}_n(k_2a) & -\mathrm{J}_n(k_1a) & -\mathrm{I}_n(k_1a) \\
k\mathrm{H}_n^{(1)\prime}(kb) & k\mathrm{K}_n'(kb) & -k_2\mathrm{Y}_n'(k_2b) & -k_2\mathrm{K}_n'(k_2b) & -k_2\mathrm{J}_n'(k_2b) & -k_2\mathrm{I}_n'(k_2b) & 0 & 0 \\
0 & 0 & k_2\mathrm{Y}_n'(k_2a) & k_2\mathrm{K}_n'(k_2a) & k_2\mathrm{J}_n'(k_2a) & k_2\mathrm{I}_n'(k_2a) & -k_1\mathrm{J}_n'(k_1a) & -k_1\mathrm{I}_n'(k_1a) \\
S_H(kb) & S_K(kb) & -S_Y(k_2b) & -S_K(k_2b) & -S_J(k_2b) & -S_I(k_2b) & 0 & 0 \\
0 & 0 & S_Y(k_2a) & S_K(k_2a) & S_J(k_2a) & S_I(k_2a) & -S_J(k_1a) & -S_I(k_1a) \\
T_H(kb) & T_K(kb) & -T_Y(k_2b) & -T_K(k_2b) & -T_J(k_2b) & -T_I(k_2b) & 0 & 0 \\
0 & 0 & T_Y(k_2a) & T_K(k_2a) & T_J(k_2a) & T_I(k_2a) & -T_J(k_1a) & -T_I(k_1a)
\end{bmatrix}$$

$$\times \begin{bmatrix} a_n \\ b_n \\ c_n \\ d_n \\ e_n \\ f_n \\ g_n \\ h_n \end{bmatrix} = - \begin{bmatrix} \mathrm{J}_n(kb) \\ 0 \\ k\mathrm{J}_n'(kb) \\ 0 \\ S_J(kb) \\ 0 \\ T_J(kb) \\ 0 \end{bmatrix}. \tag{3}$$

In equation (3) the quantities S_X and T_X, where X denotes the type of Bessel function, are defined as follows [10]:

$$S_X(\kappa) = D[n^2(1-\nu)] \mp \kappa^2]X_n(\kappa) - D(1-\nu)\kappa X_n'(\kappa),$$

$$T_X(\kappa) = D[n^2(1-\nu)]X_n(\kappa) - D[n^2(1-\nu) \pm \kappa^2]\kappa X_n'(\kappa), \tag{4}$$

where D and ν denote the appropriate flexural rigidity and the Poisson ratio for the zone being considered, κ denotes kb, k_1a, k_2a, or k_2b, and the upper (lower) signs refer to $X = \mathrm{H}^{(1)}$, J, Y, (I, K) respectively.

2.2. FREE EDGE AT INNER ZONE: HOLE

In this case, the same conditions of continuity hold on $r = b$ but M_r and V_r are set to 0 on $r = a$. The 8×8 system (3) consequently reduces to the 6×6

system

$$\begin{bmatrix} \mathrm{H}_n^{(1)}(kb) & \mathrm{K}_n(kb) & -\mathrm{Y}_n(k_2b) & -\mathrm{K}_n(k_2b) & -\mathrm{J}_n(k_2b) & -\mathrm{I}_n(k_2b) \\ k\mathrm{H}_n^{(1)\prime}(kb) & k\mathrm{K}_n'(kb) & -k_2\mathrm{Y}_n'(k_2b) & -k_2\mathrm{K}_n'(k_2b) & -k_2\mathrm{J}_n'(k_2b) & -k_2\mathrm{I}_n'(k_2b) \\ S_H(kb) & S_K(kb) & -S_Y(k_2b) & -S_K(k_2b) & -S_J(k_2b) & -S_I(k_2b) \\ 0 & 0 & S_Y(k_2a) & S_K(k_2a) & S_J(k_2a) & S_I(k_2a) \\ T_H(kb) & T_K(kb) & -T_Y(k_2b) & -T_K(k_2b) & -T_J(k_2b) & -T_I(k_2b) \\ 0 & 0 & T_Y(k_2a) & T_K(k_2a) & T_J(k_2a) & T_I(k_2a) \end{bmatrix} \begin{bmatrix} a_n \\ c_n \\ e_n \\ f_n \\ g_n \\ h_n \end{bmatrix} = - \begin{bmatrix} \mathrm{J}_n(kb) \\ k\mathrm{J}_n'(kb) \\ S_J(kb) \\ 0 \\ T_J(kb) \\ 0 \end{bmatrix}. \tag{5}$$

2.3. CLAMPED EDGE AT INNER ZONE

Here the same conditions of continuity hold on $r = b$ but now w and $\partial w/\partial r$ are set to 0 on $r = a$ with M_r and V_r unconstrained. The 8×8 system (3) then reduces to a 6×6 system as follows:

$$\begin{bmatrix} \mathrm{H}_n^{(1)}(kb) & \mathrm{K}_n(kb) & -\mathrm{Y}_n(k_2b) & -\mathrm{K}_n(k_2b) & -\mathrm{J}_n(k_2b) & -\mathrm{I}_n(k_2b) \\ 0 & 0 & \mathrm{Y}_n(k_2a) & \mathrm{K}_n(k_2a) & \mathrm{J}_n(k_2a) & \mathrm{I}_n(k_2a) \\ k\mathrm{H}_n^{(1)\prime}(kb) & k\mathrm{K}_n'(kb) & -k_2\mathrm{Y}_n'(k_2b) & -k_2\mathrm{K}_n'(k_2b) & -k_2\mathrm{J}_n'(k_2b) & -k_2\mathrm{I}_n'(k_2b) \\ 0 & 0 & k_2\mathrm{Y}_n'(k_2a) & k_2\mathrm{K}_n'(k_2a) & k_2\mathrm{J}_n'(k_2a) & k_2\mathrm{I}_n'(k_2a) \\ S_H(kb) & S_K(kb) & -S_Y(k_2b) & -S_K(k_2b) & -S_J(k_2b) & -S_I(k_2b) \\ T_H(kb) & T_K(kb) & -T_Y(k_2b) & -T_K(k_2b) & -T_J(k_2b) & -T_I(k_2b) \end{bmatrix} \begin{bmatrix} a_n \\ b_n \\ c_n \\ d_n \\ e_n \\ g_n \end{bmatrix} = - \begin{bmatrix} \mathrm{J}_n(kb) \\ 0 \\ k\mathrm{J}_n'(kb) \\ 0 \\ S_J(kb) \\ T_J(kb) \end{bmatrix}. \tag{6}$$

3. RESULTS

It is straightforward to solve systems (3), (5) and (6) using MATLAB or another application. In this work, after first conditioning the matrix, we use MATLAB to obtain the values for the unknown coefficients $a_n - h_n$.

Noting that our terms differ by a factor of $\varepsilon_n \mathrm{i}^n$ from those of reference [10], the farfield scattered amplitude arising from a wave travelling in the x direction is

$$f(\theta) = \frac{1}{\sqrt{\pi k}} \sum_{n=0}^{\infty} a_n \varepsilon_n \cos n\theta \tag{7}$$

and in common with these authors we investigate the magnitude of this function along the line $\theta = \pi$, i.e., the backscattered amplitude, normalized with respect to the square root of the inner radius a, is given as

$$\frac{|f(\pi)|}{\sqrt{a}} = \frac{2}{\sqrt{ka\pi}} \left| 1 + 2 \sum_{n=1}^{\infty} a_n (-1)^n \right|. \tag{8}$$

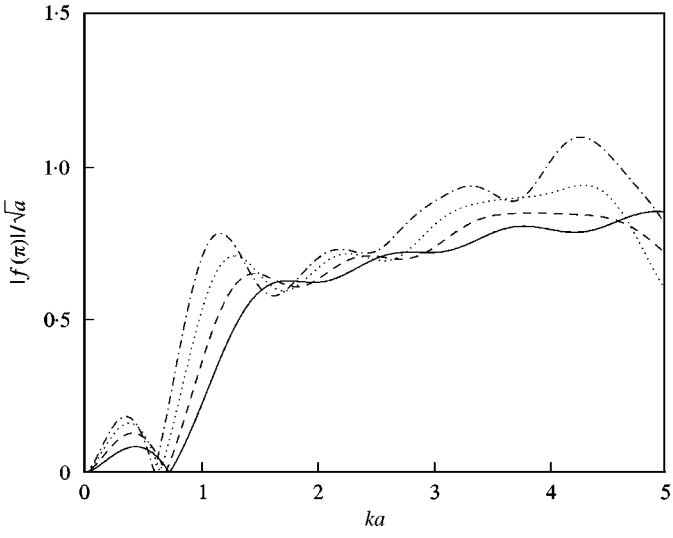

Figure 2. Normalized backscattered amplitude for a plate with a hole surrounded by a coating of twice the radius with the same thickness (solid curve) after [10], 0·9 times the thickness (dashed), 0·8 times the thickness (dotted), and 0·7 times the thickness (chained).

It is found that eight terms in the summations (1), (7) and (8) are sufficient to obtain a stable solution.

In Figure 2 we have used equation (5) to plot expression (8) for the uncoated hole, together with three other cases $h_2/h = 0{\cdot}9$, 0·8, and 0·7. The uncoated solution, drawn as a solid curve, is identical to that of reference [10], rising from zero at the origin to a low peak before dropping back to zero again and then rising steadily with ka. In the limit as $ka \to 0$ the scatterer is invisible to the very long waves and so $|f(\pi)|/\sqrt{a} \to 0$. On the other extreme, $|f(\pi)|/\sqrt{a} \to 1$ as $ka \to \infty$ because the reflection coefficient of a free edge is 1. Some fine structure is evident on the curve. The other curves are exaggerated versions of the uncoated case with more substantial fluctuations and a first minimum that moves gradually left as the coating thickness becomes less. The fluctuations grow markedly as the thickness of the coating is made less, deviating wildly from the mean trend when it is thin enough to behave as a membrane where discrete resonances occur at certain values of ka.

In Figure 3 the analogous curves are plotted for a rigid inclusion using equations (6) and (8). Again the solid curve corresponding to no coating is identical to that of reference [10]. While the high wave number limit of $|f(\pi)|/\sqrt{a}$ is still 1 because the reflection coefficient from a rigid boundary is 1, $|f(\pi)|/\sqrt{a} \to \infty$ as $ka \to 0$. Fluctuations about the mean trend appear on the curve when a coating is included, again deviating most significantly when the coating deviates most in thickness from the rest of the plate. In contrast to the curves for a hole (Figure 2), in this case the fluctuations become larger as the coating on the rigid inclusion increases.

The final simulation is carried out for a plane flexural wave impinging on (a) an unstepped and a stepped indentation, and (b) an unstepped and a stepped protrusion. Results are shown in Figure 4, where the simpler unstepped situation is shown as a solid curve in each case. In the upper plot (a) the solid curve is identical to that shown in reference [10], with a sequence of maxima separated by troughs at which little or no energy is backscattered. When a step is added the curve is similar but a little more disordered for changes in ka. The magnitude of the farfield backscattered response for the flexible

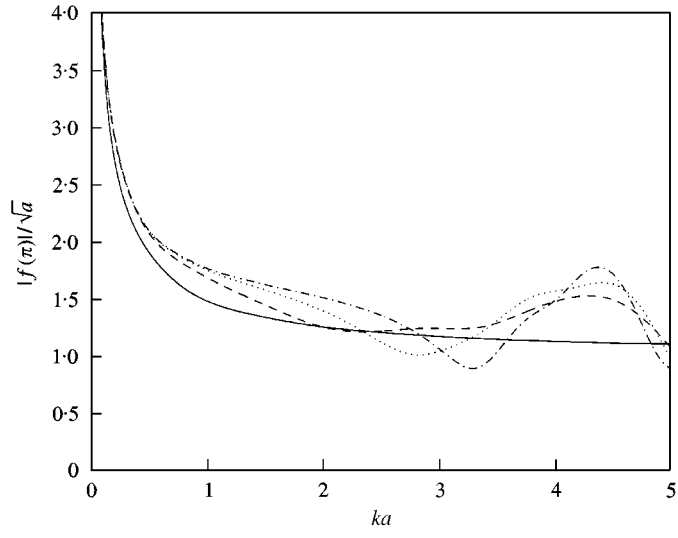

Figure 3. Normalized backscattered amplitude for a plate with a rigid inclusion surrounded by a coating of twice the radius with the same thickness (solid curve) after [10], twice the thickness (dashed), three times the thickness (dotted), and four times the thickness (chained).

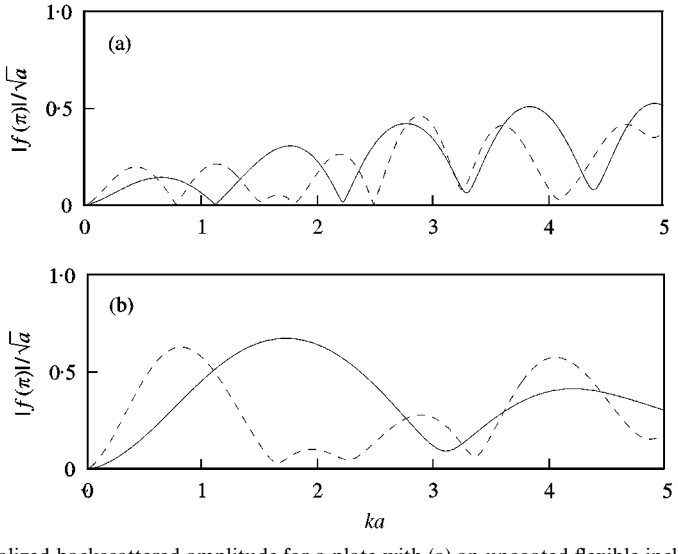

Figure 4. Normalized backscattered amplitude for a plate with (a) an uncoated flexible inclusion with $h_1 = \frac{1}{2}h$ (solid curve) after [10], and an identical inclusion surrounded by a coating with $h_2 = \frac{3}{4}h$ (dashed); (b) an uncoated flexible inclusion with $h_1 = 2h$ (solid curve) and an identical inclusion surrounded by a coating with $h_2 = 1{\cdot}5\,h$ (dashed).

protrusion is shown in the lower plot (b). Each curve is qualitatively similar to those for the inclusion but the minima are more widely separated along the ka axis.

4. CONCLUSIONS

The straightforward problem of a plane flexural wave interacting with a solitary, coated cylindrical anomaly has been solved as a series expansion of Bessel functions. It is found

that the results are consistent with those for the uncoated anomaly solved in reference [10], which serves as a check on the calculations.

In general Figures 2–4 illustrate how much fine structure can arise when rather small changes in the thickness or other properties of the coating medium are present. In part, for the cases presented this is due to the cubic dependence of the flexural rigidities D, D_1 and D_2 on thickness, and more moderate changes between curves would occur due to variations in Young's modulus, the Poisson ratio, or density. However, recall that the work reported here is a necessary precursor to modelling multiply scattered flexural wave propagation through a plate with many, randomly located, circular inclusions [3]. These may be holes, rigid or flexible protrusions, or indentations. The background medium, i.e., its thickness h, rigidity D and the Poisson ratio v, is not specified; it is computed, for example by matching energy densities [5]. Accordingly, the significant variations with ka that we are typically observing due to a change in the relative thicknesses h_2/h and h_1/h will be carried over into results obtained using CPA.

ACKNOWLEDGMENT

The work described in this paper was supported by a Marsden Grant administered by the Royal Society of New Zealand.

REFERENCES

1. D. S. Wiersma, P. Bastolini, A. Lagendijk and R. R. Righini 1997 *Nature* **390**, 671–673. Localization of light in a disordered medium.
2. P. Sheng (editor) 1990 *Scattering and Localization of Classical Waves in Random Media*. Singapore: World Scientific.
3. T. W. Dixon and V. A. Squire 2000 *Waves in Random Media* **10**, 83–102. Energy transport velocity of flexural waves in a random medium.
4. P. Sheng 1995 *Introduction to Wave Scattering, Localization and Mesoscopic Phenomena*. New York: Academic Press.
5. K. Busch and C. M. Soukoulis 1995 *Physical Review Letters* **75**, 3442–3445. Transport properties of random media: a new effective medium approach.
6. H. P. Schreimer, M. L. Cowan, J. H. Page, P. Sheng, Z. Liu and D. A. Weitz 1997 *Physical Review Letters* **79**, 3166–3169. Energy velocity of diffusing waves in strongly scattering media.
7. H. P. Schreimer, M. L. Cowan, J. H. Page, P. Sheng, Z. Liu and D. A. Weitz 1999 *Physical Review Letters* **82**, 2001–2001. Energy velocity of diffusing waves in strongly scattering media.
8. C. M. Soukoulis, K. Busch, M. Kafesaki and E. N. Economou 1999 *Physical Review Letters* **82**, 2000–2000. Comment on 'Energy velocity of diffusing waves in strongly scattering media'.
9. A. L. Aden and M. Kerker 1951 *Journal of Applied Physics* **22**, 1242–1246. Scattering of electromagnetic wave from two concentric spheres.
10. A. N. Norris and C. Vemula 1995 *Journal of Sound and Vibration* **181**, 115–125. Scattering of flexural waves on thin plates.